

## Synthesis of a New DPTYEAP Ligand and Its Complexes with Their Assessments on Physical Properties, Antioxidant, and Biological Potential to Treat Breast Cancer

Abbas Fadhil Yasir\* and Hayder Obaid Jamel

Department of Chemistry, College of Education, University of Al-Qadisiyah, 58001 Al-Diwaniyah, Iraq

\* Corresponding author:

email: abbas9025@gmail.com

Received: January 26, 2023

Accepted: February 17, 2023

DOI: 10.22146/ijc.81734

**Abstract:** A new series of complexes of the 2-((1E,2E)-1,2-diphenyl-2-(thiazol-2-ylimino)ethylidene)amino)phenol (DPTYEAP) has been synthesized by the reaction of the ligand with metal chlorides of Ni(II), Cu(II), Pt(IV), and AgNO<sub>3</sub> in ethanol as a solvent. The ligand was prepared for the two steps. In the first step, compound (A) was synthesized by reacting 2-aminothiazol with benzil in ethanol. Another step is the preparation of the ligand from the reaction of compound (A) with 2-aminophenol. The structures of the ligand and its complexes were confirmed by FTIR, <sup>1</sup>H-<sup>13</sup>C-NMR, UV-Vis spectra, melting points, molar conductivity (C, H, and N), and magnetic susceptibility. The synthesized complexes were prepared in a 1:2 ratio for Ni(II), Cu(II), and Pt(IV) complexes and a 1:1 ratio (M:L) for Ag(I) complexes. The geometric shape of all complexes is octahedral, except for the Ag(I) complex, which is tetrahedral. The antioxidant test for the prepared compounds was carried out. The anticancer test was conducted for each of the ligands and the platinum(IV) complex, and it was found that the platinum complex is more effective against breast cancer cells (MCF-7); thus, it can be used as a potential drug after studying it well.

**Keywords:** Schiff base; 2-aminothiazoles; anticancer; antioxidant; platinum(IV)

### ■ INTRODUCTION

Breast cancer occurs when some of the breast cells begin to grow abnormally. These cells divide more rapidly than healthy cells and continue to accumulate, forming a lump or tumor [1]. The cells may spread through the breast to the lymph nodes or other body parts [2]. Breast cancer comes after skin cancer as the most common type of cancer among women [3]. Breast cancer sometimes affects both men and women, but it is more common in women. Substantial support for breast cancer awareness and research funding has helped advance breast cancer diagnosis and treatment [4]. Breast cancer survival rates have increased, and the number of deaths associated with this disease has regularly decreased, largely due to several factors, such as early detection and a better understanding of the nature of this disease.

Among the used treatments, the thiazole compound had an important and effective role in preparing many anti-breast cancer complexes, especially when it is linked to platinum [5]. One of the drugs containing thiazoles,

which has been used as an anti-cancer compound, is Bleomycin [6]. The 2-aminothiazole compound is effective in treating and controlling breast cancer, in addition to its various and wide applications in various fields, especially in the pharmaceutical industry. Amino-thiazole is recently identified as a desirable compound; it has been diagnosed and examined in many medicinal chem drugs because of its thiourea-like properties and its tendency to target multiple biological targets [7]. It has also been used as an anti-bacterial [8], an antioxidant, an anti-viral [9], and a fungicide [10]. 2-Amino-thiazole and its derivatives have a wide range of medical applications as well, such as anti-tuberculosis [11], anti-inflammatory [12], anti-platelet, and are used as anti-tumors [13]. This study observed that the prepared ligand derived from amino thiazoles and its platinum(IV) complex had high antioxidant activity against free radicals. As well as high effectiveness against breast cancer cells (MCF-7), and this has been proven through applications and examinations conducted on them, which

can be used as an anti-cancer treatment. In addition, they are considered nanocomposites after confirming this through the XRD and FESEM tests. This characteristic makes these compounds could be used in many fields, including the medical and industrial fields [14].

## ■ EXPERIMENTAL SECTION

### Materials

In this study, 2-amino thiazoles (98% purity, Merck), benzil (98%, Sigma-Aldrich), acetic acid (99%, BDH), and 2-aminophenol (99%, Sigma-Aldrich) were used. At the same time, all metal chlorides (platinum(IV), nickel(II), copper(II)), and silver nitrate) were brought from Sigma-Aldrich. They were of varying purity 99.9, 98, 97.5, and 99%, respectively. Also, the study used free radical 1,1-diphenyl-2-picrylhydrazyl, supplied by Sigma-Aldrich for an antioxidant check. Breast cancer cell lines (MCF-7) and normal cell lines (WRL-68) were obtained from the Center for Natural Product Research and Drug Discovery, Department of Pharmacology, Faculty of Medicine, University of Malaya, Kuala Lumpur.

### Instrumentation

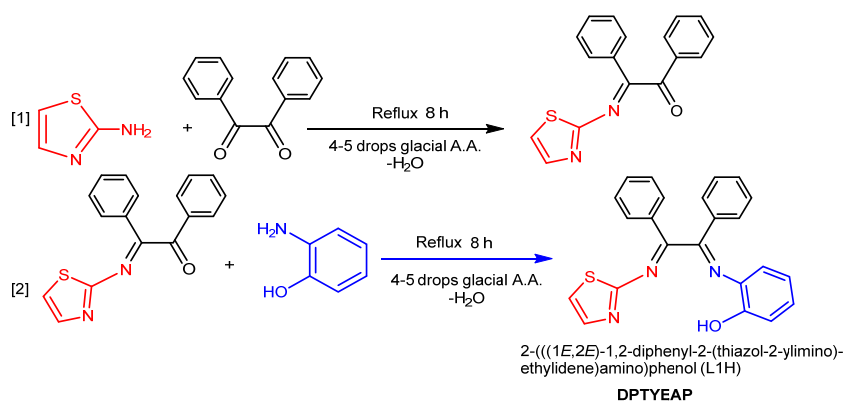
UV-Vis spectra in the region of 200–1000 nm were obtained using Shimadzu UV-165 PCS spectrophotometer. On the Fourier Transform Varian Spectrometer,  $^1\text{H}$ ,  $^{13}\text{C}$ -NMR spectra were acquired at 300 MHz with tetramethyl silane as a standard internal reference in DMSO- $d_6$  solvent. The FTIR 8400S Shimadzu Spectrophotometer was used to record FTIR Spectra in the 400–4000  $\text{cm}^{-1}$  range. The Stuart melting point was used to determine the melting points of all compounds.

At room temperature, magnetic susceptibility measurements were taken using the Balance Magnetic Susceptibility Model MSB-MKI; flame atomic absorption spectrophotometer, Shimadzu AA-6300 was used to determine metal percentage in the complexes; Elemental analysis was recorded on instrument type EA-300.mth.

### Procedure

#### Preparation of the ligand DPTYEAP

The ligand was prepared in two steps. The first step was the preparation of (*E*)-1,2-diphenyl-2-(thiazol-2-ylimino)ethan-1-one (compound-A) from the reaction between 2-aminothiazol (2.002 g, 0.02 mol) in 25 mL of the absolute ethanol with benzil (4.204 g, 0.02 mol) in 25 mL ethanol with a continuous stirring. The mixture was refluxed for 8 h. After that, it was cooled, filtered, and collected. It was recrystallized by removing the residue of the starting material with 99.9% ethanol, allowing the precipitate to dry; then, it will be collected and weighed to be employed in the second stage, yielding an 84% yield percentage. The ligand 2-(((1*E*,2*E*)-1,2-diphenyl-2-(thiazol-2-ylimino)ethylidene)amino)phenol (DPTYEAP) was prepared by dissolving compound-A (4.385 g, 0.015 mol) in 25 mL of ethanol with a solution of 2-aminophenol (1.636 g, 0.015 mmol) in 25 mL of ethanol. Then, 5–6 drops of concentrated hydrochloric acid were added to the mixture with continuous stirring, the mixture was refluxed for 8 h. It was cooled, precipitated, filtered, dried, and recrystallized by using absolute ethanol. The product gave a yield of 79%, and a melting point of 113 °C, as stated in Scheme 1.



**Scheme 1.** Synthesis of the 2-(((1*E*,2*E*)-1,2-diphenyl-2-(thiazol-2-ylimino)-ethylidene)amino)phenol (DPTYEAP) ligand

### Synthesis of the complexes

Two types of the complex are prepared with a ratio of 1:1 and 1:2, which are as follows:

**Preparation of Ni(II), Cu(II), Pt(IV) complexes with DPTYEAP ligand.** These complexes were prepared in 1:2 using the following general method. A solution of DPTYEAP ligand (1.533 g, 0.004 mol) in 10 mL ethanol was mixed with 0.002 mol of metal chlorides in 10 mL of absolute ethanol. The mixture was refluxed for 2 h while stirring. After that, it was cooled, filtrated, and dried before re-crystallized using absolute ethanol to obtain pure complexes.

**Preparation of Ag(I) complexes with DPTYEAP ligand.** The above complex was made using the same method but in a different ratio 1:1 M:L. DPTYEAP ligand solution (0.766 g, 0.002 mol) in 10 mL ethanol was added to silver nitrate solution (0.339 g, 0.002 mol) in 10 mL absolute ethanol. The mixture was refluxed for 2 h with stirring before being cooled, filtrated, and dried.

### Measuring antioxidant capacity

The concentration of the tested compound which causes 50% of radical scavenging activity ( $IC_{50}$ ) was determined by the linear regression analysis from the obtained RSA values using GraphPad Prism 8.3.1 software. DPTYEAP ligand and metal complexes were tested for radical scavenging activity against DPPH using a spectrophotometric method. In practice, 1 mL of the ligand and metal complexes in DMSO at various concentrations 3.90–500 g/mL was mixed with 1 mL of 0.1 mM DPPH in methanol. For 30 min, the tested samples were allowed to react with DPPH. After 30 min of incubation in the darkness at room temperature, the absorbance at 517 nm was measured with Shimadzu UV-165PCS spectrophotometer. Then, the RSA% was calculated. The linear regression analysis was performed on the obtained RSA values to determine the  $IC_{50}$  value. The lower the value of  $IC_{50}$ , the more efficient the antioxidant [15].

### Biological activity (Cytotoxic assay MTT)

In this study, two cell lines were used, namely the breast cancer cell line (MCF-7) and the normal human liver cell line (WRL-68). Cell lines were preserved in liquid nitrogen and were maintained and tested at the Biotechnology Research Center - Al-Nahrain University.

After the cells of cancer lines (MCF-7) and the suspension were prepared at a concentration of  $1 \times 10^5$  cells/well completely, the cell suspension was placed in a plate containing 96 holes with a flat base, and it was incubated in an incubator with 5% carbon dioxide ( $CO_2$ ) at a temperature of 37 °C, for 24 h. Then, 100  $\mu$ L of this suspension was added to each well. After that, the concentrations that had been prepared for each of the ligands and the platinum complex 25, 50, 100, 200, and 400  $\mu$ g/mL were added to those wells at the rate of three wells for each concentration. After that, the plate was incubated for a full day at an incubation temperature of 37 °C, and 10 mL of MTT solution at a concentration of 0.45 mg/mL was added to each hole. Then that plate was incubated for 4 h at 37 °C. 100  $\mu$ L of DMSO solution was added to each hole and incubated for 5 min [16]. Finally, the absorbance of that sample was read at a wavelength of 570 nm using the ELASIS device, then the statistical analysis was conducted on the optical density readings to calculate the  $IC_{50}$ .

## RESULTS AND DISCUSSION

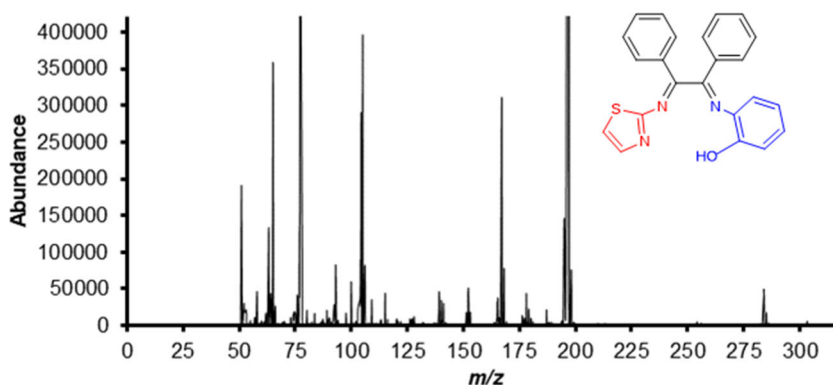
The new ligand (DPTYEAP) was synthesized from the consecutive reaction of 2-aminothiazol with benzil and 2-aminophenol. The complexes have been prepared from the reaction of DPTYEAP with metal chlorides hydrates and  $AgNO_3$  dissolved in ethanol. Table 1 shows the physical attributes and elemental analyses for each of the ligands and the complexes. The synthesized complexes were created in a 1:2 ratio for Ni(II), Cu(II) and Pt(IV) complexes, whereas Ag(I) complex was prepared in a 1:1 ratio (M:L).

### Mass Spectrum of the DPTYEAP Ligand

It is one of the analytical techniques used in an accurate diagnosis to determine the prepared compound and what elements are present in its composition, as well as its molecular and structural formula. The idea behind its operation is to break the compound into ions, after which the mass-to-charge ratio is measured using a mass spectrometer. Fig. 1 shows the DPTYEAP ligand fragmentation with the appearance of a peak for the parent ion at  $m/z^+ = 383.99$ , as well as the rest of the divisions.

**Table 1.** Elemental analysis and some physical properties of the ligand (DPTYEAP) and its metallic complexes

Compound (Chemical Formula)	Color	M P (°C)	Yield (%)	M.W (g/mol)	Calc. (Found)%			
					C	H	N	M
Ligand (DPTYEAP) (C <sub>23</sub> H <sub>17</sub> N <sub>3</sub> OS)	Brown	113		383.50	71.55 (72.04)	4.12 (4.47)	8.90 (10.96)	-----
[Ni (DPTYEAP) <sub>2</sub> ].H <sub>2</sub> O (C <sub>46</sub> H <sub>34</sub> N <sub>6</sub> NiO <sub>3</sub> S <sub>2</sub> )	Dark green	120		841.63	64.18 (65.65)	4.43 (4.07)	8.18 (9.99)	5.65 (6.97)
[Cu (DPTYEAP) <sub>2</sub> ].H <sub>2</sub> O (C <sub>46</sub> H <sub>34</sub> CuN <sub>6</sub> O <sub>3</sub> S <sub>2</sub> )	Dark brown	118		846.48	63.32 (65.27)	3.80 (4.05)	8.11 (9.93)	6.98 (7.51)
[Ag (DPTYEAP) H <sub>2</sub> O] (C <sub>23</sub> H <sub>18</sub> AgN <sub>3</sub> O <sub>2</sub> S)	Yellowish green	123		508.34	61.09 (54.34)	3.79 (3.57)	7.98 (8.27)	20.17 (21.22)
Pt[(DPTYEAP) <sub>2</sub> ].Cl <sub>2</sub> .H <sub>2</sub> O (C <sub>46</sub> H <sub>34</sub> Cl <sub>2</sub> N <sub>6</sub> O <sub>3</sub> PtS <sub>2</sub> )	Dark golden	117		1048.92	52.03 (52.67)	3.03 (3.27)	6.67 (8.01)	17.97 (18.60)

**Fig 1.** Mass spectrum of Schiff base DPTYEAP ligand

### The <sup>1</sup>H-NMR spectra of the DPTYEAP ligand

The <sup>1</sup>H-NMR Spectrum of the DPTYEAP ligand exhibited a singlet signal at  $\delta = 8.655$  ppm (s, 1H) due to hydroxide proton (OH) [17], while the multiple signals were observed at the range  $\delta = 6.986$ –7.438 ppm (m, 4H) due to the 2-aminophenol ring protons [18]. Where the multiple signals at  $\delta = 7.456$ –7.793 ppm (m, 5H) and  $\delta = 7.464$ –7.837 ppm (m, 5H) are attributed to rings protons found in benzil [19]. While the doublet signals at  $\delta = 7.166$ –7.545 ppm (d, 2H) are attributed to ring protons found in thiazole [20]. Fig. 2 shows the <sup>1</sup>H-NMR spectra of the DPTYEAP ligand.

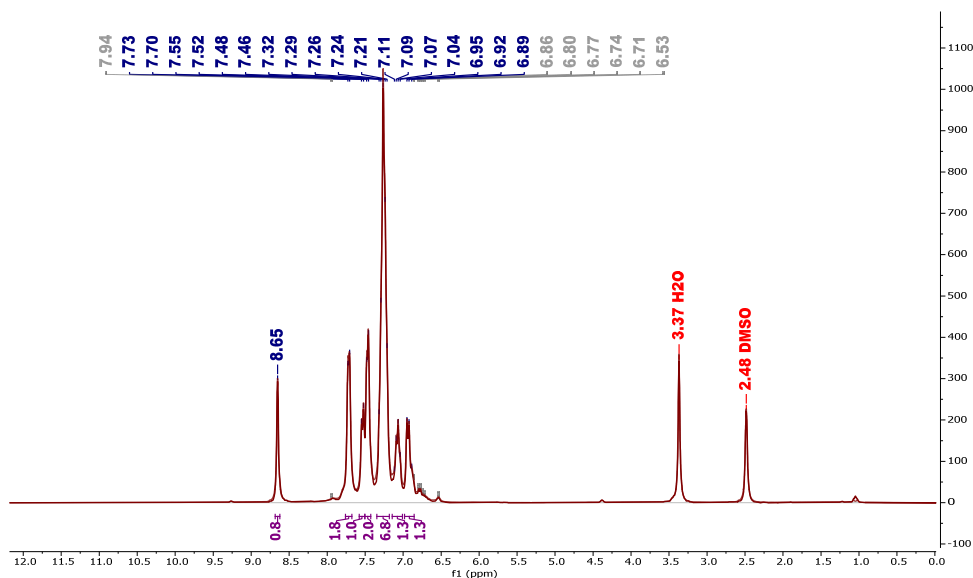
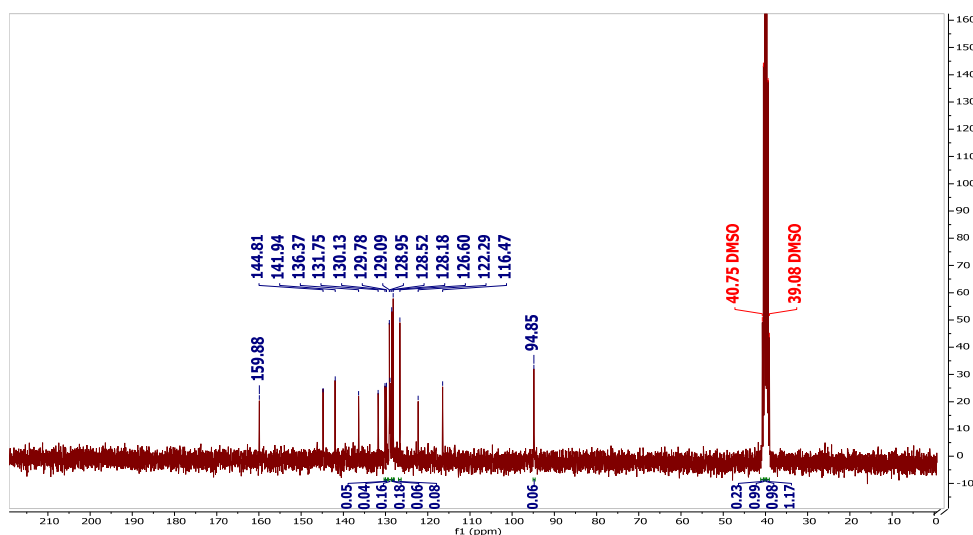
### The <sup>13</sup>C-NMR spectrum of the ligand (DPTYEAP)

The <sup>13</sup>C-NMR Spectrum of the ligand DPTYEAP exhibited a signal at 40.311 ppm, due to DMSO. The carbon C<sub>23</sub> containing the group OH gave a signal at 136.648 ppm [21], while the carbon C<sub>9</sub> gave the signal at 116.476 ppm due to thiazole [22]. Where the following

carbon atoms C<sub>3</sub>–C<sub>4</sub>–C<sub>10</sub>–C<sub>22</sub> gave values between 129.092–131.752 ppm due to the connection of carbon atoms with nitrogen atoms [23–24]. As for these two signals at 144.818–141.912 ppm, C<sub>1</sub>–C<sub>2</sub> is due to the two groups of azomethane (–C=N–) [25]. Several signals at 129.275–129.627, 129.000–129.927, and 115.742–124.927 ppm indicated the carbon atoms C<sub>12</sub>–C<sub>16</sub>, C<sub>17</sub>–C<sub>21</sub>, and C<sub>24</sub>–C<sub>27</sub> belong to the phenyls of benzil and phenol, respectively [26]. Fig. 3 shows the <sup>13</sup>C-NMR spectra of the DPTYEAP ligand.

### The Infrared Spectra

Diagnosis of free ligand DPTYEAP by infrared spectrometer for the purpose of determining the effective groups. The ligand showed many important bands at the wavenumber 3425, 3062, and 1666 cm<sup>-1</sup> belonging to the  $\nu$ (O–H),  $\nu$ (C–H) aromatic [27], and  $\nu$ (C=N) azomethine, respectively [28], as shown in (Fig. S2).

Fig 2.  $^1\text{H-NMR}$  spectra of the DPTYEAP ligandFig 3.  $^{13}\text{C-NMR}$  spectra of the DPTYEAP ligand

### The infra-red spectra of the complexes

When following up the spectrum of the prepared DPTYEAP ligand complexes and comparing it with the spectrum of the free ligand, all the spectra were clarified in Fig. S3–S6. There was a displacement of some bands and the disappearance of others, as well as the emergence of new bands, which are shown in Table 2. These all indicate the occurrence of coordination between the ionic metals and ligands. The most important indication for the coordination between the ligand and the metals is the disappearance of the hydroxyl band in the prepared complexes [29], as well as the displacement of the azomethine group belonging to the Schiff base towards

the lower frequencies by 6–10  $\text{cm}^{-1}$  compared to the ligand spectrum [30], while there was the emergence of new bands of the hydroxyl group belonging to the water molecules of crystallization [31].

### Electronic Spectra

The spectrum of the free ligand DPTYEAP derived from 2-aminothiazole in the spectrophotometer showed three absorption peaks, each of them at 47393, 40322, and 39525  $\text{cm}^{-1}$ , which gave transitions of the type  $\pi-\pi^*$  and  $n-\pi^*$  belonging to each of the phenyl rings and azomethine groups ( $\text{C}=\text{N}$ ), respectively [32]. Fig. S7 shows the absorption peaks of the free ligand.

**Table 2.** The important infrared spectral bands for the synthesized ligand (DPTYEAP) and its metallic complex

Compound	$\nu(\text{O-H})$ of water molecules	$\nu(\text{O-H})$	$\nu(\text{C-H})$ aromatic	$\nu(\text{C=N})$		$\nu(\text{M-N})$	$\nu(\text{M-O})$
				Imine	Thiazole		
Ligand (DPTYEAP)	-----	3425 (bro)	3062 (w)	1666 (s)	1596 (s)	-----	-----
[Ni(DPTYEAP) <sub>2</sub> ].H <sub>2</sub> O	3348 (bro)	-----	3062 (w)	1660 (s)	1595 (s)	563 (w)	432 (m)
[Cu(DPTYEAP) <sub>2</sub> ].H <sub>2</sub> O	3317 (bro)	-----	3062 (w)	1657 (s)	1596 (s)	578 (w)	462 (s)
[Ag (DPTYEAP) H <sub>2</sub> O]	3464 (bro)	-----	3062 (w)	1658 (w)	1596 (s)	547 (m)	470 (s)
Pt[(DPTYEAP) <sub>2</sub> ]Cl <sub>2</sub> .H <sub>2</sub> O	3379 (bro)	-----	3062 (w)	1661 (s)	1594 (s)	547 (w)	424 (s)

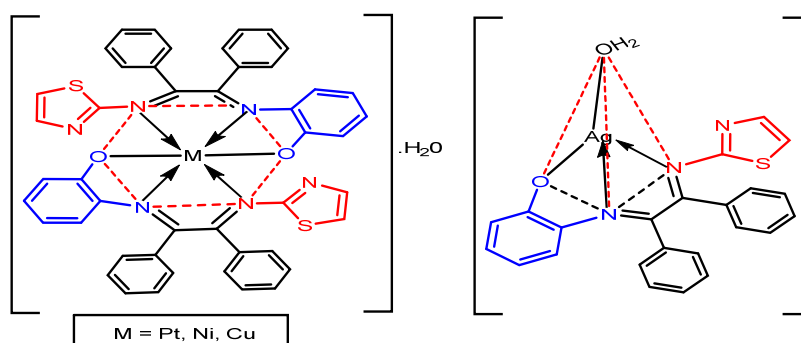
### The electronic spectra of the synthesized metallic complexes

The spectrum of the Ni(II) complex showed five absorption peaks, two of which belong to the ligand field, which are 46296 and 38610 cm<sup>-1</sup>. While the next three absorption peaks at 16920, 16207, and 15923 cm<sup>-1</sup> indicate the following transitions <sup>3</sup>A<sub>2g</sub> (P) → <sup>3</sup>T<sub>1g</sub> (F), <sup>3</sup>A<sub>2g</sub> (F) → <sup>3</sup>T<sub>2g</sub> (F), <sup>3</sup>A<sub>2g</sub> (F) → <sup>3</sup>T<sub>1g</sub> (F), respectively, as in Fig. S8 [33]. While the spectrum of the Cu(II) complex showed three absorption peaks, which are 46948, 37878, and 18450 cm<sup>-1</sup>, two of them belong to the ligand field, and the last one belongs to the <sup>2</sup>B<sub>1g</sub> → <sup>2</sup>E<sub>g</sub> transition, as in Fig. S9 [34]. While the spectrum of Ag(I) complex did not show any transitions (d-d) due to the saturation of the metal with electrons, and at the same time, it showed three absorption peaks, which are 46511, 38167, and 27548 cm<sup>-1</sup> two of them belong to the ligand field. The last peak belongs to the M-L charge transitions as in Fig. S10 [35]. The Pt(IV) complex showed five absorption peaks, which are 47169, 38461, 24154, 18726, and 13679 cm<sup>-1</sup>; two belong to the ligand field and

three belong to the transitions of <sup>1</sup>A<sub>1g</sub> → <sup>1</sup>T<sub>1g</sub>, <sup>1</sup>A<sub>1g</sub> → <sup>1</sup>T<sub>2g</sub> respectively as in Fig. S11 [36]. Table 3 shows the electronic transitions, the geometric shape, as well as the magnetic sensitivity. It turned out that the geometric shape of all complexes is octahedral, except for the Ag(I) complex, which is tetrahedral. Fig. 4 shows the proposed chemical structure formula of the complexes.

### Molar Conductivity

In coordination chemistry, the electrical conductivity technique was used for the purpose of knowing the ionic formula of the prepared ligand complexes and that the conductivity depends on the number of ions present in the solution as well as the concentration so that when the crystal molar conductivity is close to zero here, the compound has a non-ionic character, and if it is greater, it is ionic. It was found that most of the prepared complexes are non-ionic while the silver complex is ionic [37], which is clarified in Table 3.

**Fig 4.** The proposed chemical structure formula of the complexes

**Table 3.** Electronic spectra, magnetic moments and molar conductivity of the DPTYEAP ligand and its metallic

Compounds	$\lambda$ (nm)	$\nu^-$ ( $\text{cm}^{-1}$ )	Transitions	$\mu_{\text{eff}}$ (B.M)	Hyperdization and Geometry	$\Lambda$ ( $\text{ohm}^{-1}$ , $\text{cm}^2, \text{mol}^{-1}$ )
DPTYEAP	211	47393	$\pi-\pi^*$			
	248	40322	$\pi-\pi^*$	-----	-----	-----
	253	39525	$n-\pi^*$			
[Ni(DPTYEAP) <sub>2</sub> ].H <sub>2</sub> O	216	46296	Ligand Field			
	259	38610	Ligand Field		$\text{sp}^3\text{d}^2$	
	591	16920	$^3\text{A}_{2g}(\text{F}) \rightarrow ^3\text{T}_{1g}(\text{P})$	3.87	Octahedral	15.8
	617	16207	$^3\text{A}_{2g}(\text{F}) \rightarrow ^3\text{T}_{2g}(\text{F})$	(Para.)	Distorted	no ionic
	628	15923	$^3\text{A}_{2g}(\text{F}) \rightarrow ^3\text{T}_{1g}(\text{F})$			
[Cu(DPTYEAP) <sub>2</sub> ].H <sub>2</sub> O	213	46948	Ligand Field			9.9
	264	37878	Ligand Field	1.74	$\text{sp}^3\text{d}^2$	no ionic
	542	18450	$^2\text{B}_{1g} \rightarrow ^2\text{E}_g$	(Para.)	Octahedral	
[Ag (DPTYEAP) H <sub>2</sub> O]	215	46511	Ligand Field		$\text{sp}^3$	10.5
	262	38167	Ligand Field	0.00	Tetrahedral	no ionic
	363	27548	Charge transfer (MLCT)	(Dia.)		
Pt[(DPTYEAP) <sub>2</sub> ] Cl <sub>2</sub> .H <sub>2</sub> O	212	47169	Ligand Field		$\text{d}^2\text{sp}^3$	37.1
	260	38461	Ligand Field		Octahedral	Ionic
	534	18726	$^1\text{A}_{1g} \rightarrow ^1\text{T}_{1g}$		Distorted	1:2
	731	13679	$^1\text{A}_{1g} \rightarrow ^1\text{T}_{2g}$			

### X-Ray Diffraction

It was found by measuring the X-ray diffraction spectra that the ligand DPTYEAP and complexes of nickel, platinum, silver, and copper have crystal structures, meaning with a crystalline level and a crystal lattice. This was also shown clearly in Fig. 5(a-e), as well as Table 4 and when comparing the intensity and locations of the peaks of the results obtained with the international standard cards, it was found that these locations belonged to the original basic compounds from which the compounds were prepared and also that the presence of any strange location or peak was not indicated or that it belongs to a substance that is not originally found in the basic compounds, and the reason is that the compounds are new and has not been compared with the various international standard cards [38]. By taking advantage of the data contained in the X-ray diffraction, it was found that the materials that were prepared can be said to be of a nanoscale nature. Fig. S12 and S13 show the XRD patterns for DPTYEAP ligand and chelate complexes.

### Scanning Electron Microscopy (FESEM)

The crystal structure of every DPTYEAP ligand and

its complexes was known and studied through the scanning microscopy technique, as well as the surface characteristics morphology, shape, and size of the particles. The ligand was discovered to have a somewhat spherical shape, and the average particle size was 69.19 nm. While the Ni(II) complexes FESEM image revealed that it was entirely spherical and homogeneous and that the average particle size was 71.57 nm. It was discovered that a FESEM image appeared for Ag(I) complexes with a granular and spherical shape and an average particle size of 86.31 nm, as well as for Pt(IV) complexes with a heterogeneous shape and average particle size of 88.67 nm. Lastly, the FESEM image of the Cu(II) complexes revealed that they have square shapes and do not qualify as a nanoscale compound. Through research on FESEM technology, it was discovered that substances with granular crystal structures, or those that fall within the nanoscale, are substances of importance because of the advantages that can be derived from them in the fields of industry, such as thermal or electrical conduction, or in the fields of medicine and pharmacology, such as the treatment of some forms of cancer or some dangerous bacteria, as shown in Fig. 5

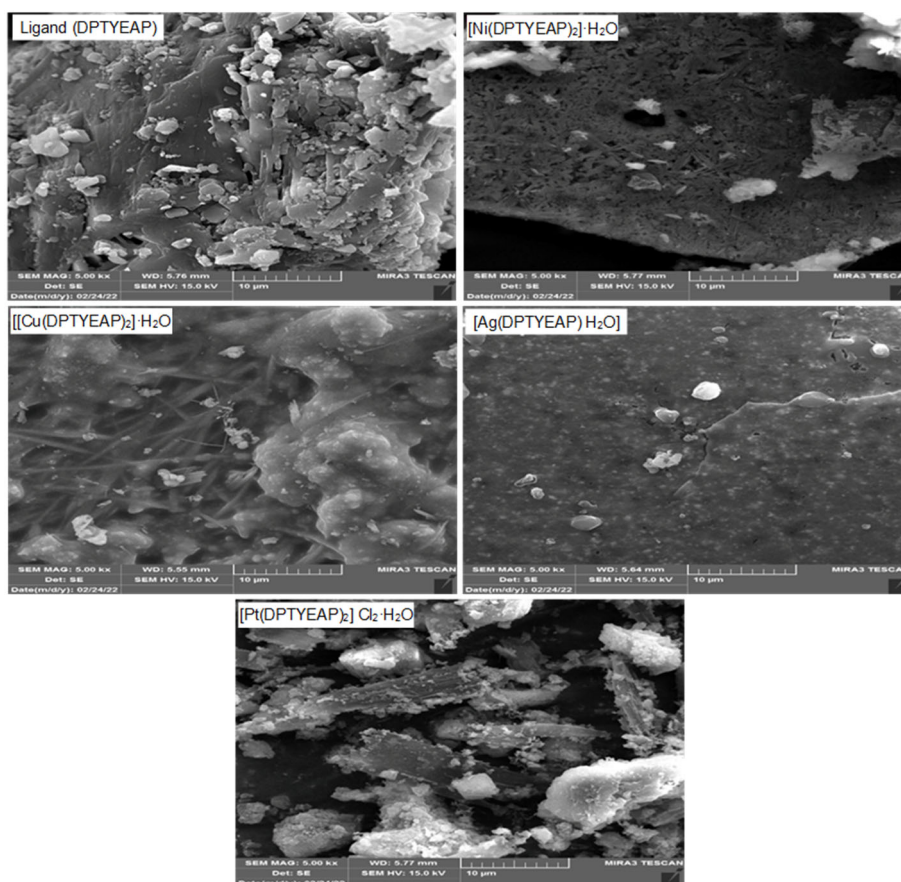


**Fig 5.** Shows the FESEM image of the (a) synthesized (DPTYEAP) ligand, (b) Ni(II) complex, (c) Cu(II) complex, (d) Ag(I) complex, and (e) Pt(IV) complex

**Table 4.** Crystallographic data for DPTYEAP ligand and its complexes

Compound	No.	Peak position $2\theta$ ( $^{\circ}$ )	Height (cts)	Peak width (FWHM)	$d$ -spacing [ $\text{\AA}$ ]	Rel. Int. (%)	D Crystal-lite size (nm)
DPTYEAP	1-	18.5074	969.3600	0.2362	4.7942	100.0000	36.5700
	2-	23.5473	579.5100	0.1968	3.7783	59.7800	43.2600
	3-	12.1177	406.1300	0.1968	7.3040	41.9000	42.4200
	4-	23.0260	385.1600	0.1574	3.8626	39.7300	53.9600
	5-	24.8659	352.8100	0.1574	3.5808	36.4000	54.1400
	6-	14.6978	348.1400	0.1181	6.0271	35.9100	70.9290
[Ni (DPTYEAP) <sub>2</sub> ].H <sub>2</sub> O	1-	25.2984	1095.5000	0.1574	3.5206	100.0000	54.1900
	2-	17.7801	610.1600	0.1574	4.9886	55.7000	53.5200
	3-	24.4030	392.7500	0.1574	3.6477	35.8500	54.1000
[Cu (DPTYEAP) <sub>2</sub> ].H <sub>2</sub> O	1-	25.2370	594.0300	0.1181	3.5290	100.0000	72.0900
	2-	24.3631	457.0400	0.1574	3.6536	76.9400	54.0890
	3-	17.7079	377.3800	0.1574	5.0088	63.5300	53.1000
[Ag (DPTYEAP)H <sub>2</sub> O]	1-	22.1160	1726.4800	0.1181	4.0194	100.0000	71.6790
	2-	25.2823	351.4500	0.1574	3.5228	20.3600	54.1900
	3-	17.7757	305.9900	0.1181	4.9899	17.7200	71.2000
[Pt (DPTYEAP) <sub>2</sub> ]Cl <sub>2</sub> .H <sub>2</sub> O	1-	38.1092	1097.3000	0.2362	2.3614	100.0000	37.1800
	2-	44.3202	367.3400	0.2362	2.0439	33.4800	37.9500
	3-	64.4137	345.4300	0.1968	1.4465	31.4800	50.0500

FESEM images of the synthesized DPTYEAP ligand and metal complexes.

## Applications

### Antioxidant activity

The anti-free radical test was carried out for each of the ligands DPTYEAP and all the prepared metal complexes used in recent years on a large scale to estimate the antioxidant activity. This test depends on the presence of an antioxidant compound that is able to donate an electron or a hydrogen radical to the compound DPPH, which has a violet color, the interaction of the prepared compounds with the compound DPPH and the disappearance of the violet color and its transformation into a more stable compound is an indication that the compounds possess high antioxidants. The measurements for each of the DPTYEAP ligands and the complexes of platinum and nickel showed a high activity of antioxidants towards DPPH. The highest inhibition percentage was reached for the prepared compounds at a concentration of 500 µg/mL, ranging between 71.43–90.83%. While the lowest inhibition percentage which was

at a concentration of 3.9 g/mL, ranged between 16.83–35.00%. The copper complex showed weak antioxidant activity towards DPPH, while the silver complex did not show any antioxidant activity. On the other hand, the value of the half inhibitory concentration  $IC_{50}$  for each of the ligand DPTYEAP and all the metal complexes under study ranged between 0.9819–1430.5430, as shown in Table 5 and Fig. 6 shows the antioxidant activity of DPPH scavenger radical for DPTYEAP ligand and its complexes. Based on the values of  $IC_{50}$ , that is the lower its value, the greater its antioxidant effectiveness, the compound's effectiveness can be arranged as follows: Ascorbic Acid > Pt[(DPTYEAP)<sub>2</sub>] > Ligand > [Ni (DPTYEAP)<sub>2</sub>] > [Cu (DPTYEAP)<sub>2</sub>] > [Ag (DPTYEAP) H<sub>2</sub>O].

### Anticancer activity

The MTT cytotoxicity assay was performed on the (MCF-7) breast cancer cell line for both the DPTYEAP ligand and the Pt(IV) complex because it is the most common type of cancer in women. In addition, the normal cell line WRL-68 was used to determine the effect of the DPTYEAP ligand and the Pt(IV) complex on

**Table 5.** Antioxidant activity from the analysis in vitro for ligand (DPTYEAP) and its metal complexes

Compound	Concentration µg/mL									$IC_{50}$
	0.00	3.90	7.81	15.62	31.25	62.50	125.00	250.00	500.00	
Ascorbic Acid	0.00	64.50	68.12	72.24	78.66	80.02	85.33	89.66	95.54	0.98
Ligand (DPTYEAP)	0.00	35.00	42.50	47.50	55.83	56.25	62.50	66.66	74.16	17.95
[Ni(DPTYEAP) <sub>2</sub> ]. H <sub>2</sub> O	0.00	25.55	35.60	38.66	45.87	49.81	55.76	59.88	71.43	102.33
[Cu(DPTYEAP) <sub>2</sub> ]. H <sub>2</sub> O	0.00	0.00	4.16	8.30	10.00	12.50	14.16	17.50	22.50	1430.54
[Ag (DPTYEAP) H <sub>2</sub> O]	0.00	0.00	0.00	0.00	0.00	0.00	0.00	0.00	0.00	-
Pt[(DPTYEAP) <sub>2</sub> ]Cl <sub>2</sub> .H <sub>2</sub> O	0.00	16.83	25.00	55.00	72.25	75.83	83.33	84.16	90.83	13.33

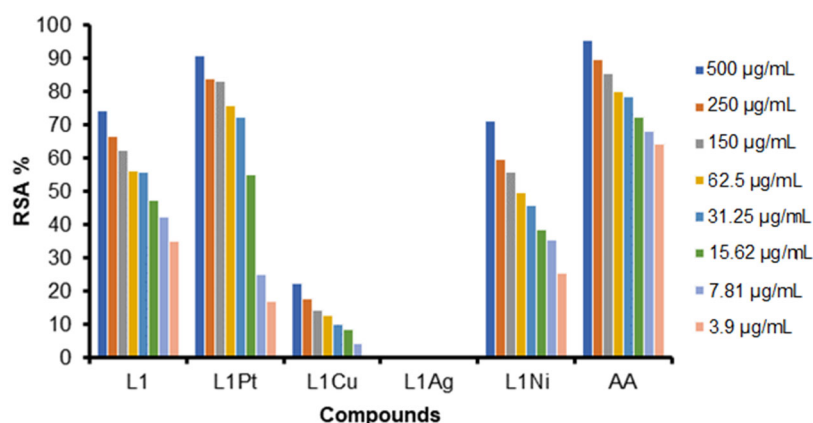


**Fig 6.** Antioxidant activity of DPPH scavenger radical for DPTYEAP ligand and its complexes

**Table 6.** Evaluation of the cytotoxicity of both the ligand and the Pt(IV) complex against the MCF-7 cancer cell line after incubation (24 h) at (37 °C)

Conc.	Viability % Mean $\pm$ SD							
	MCF-7 L1	Inhibition of dead cells % MCF-7	WRL-68 L1	Inhibition of dead cells % WRL-68	MCF-7 L1Pt	Inhibition of dead cell % MCF-7	WRL-68 L1Pt	Inhibition of dead cells % WRL-68
400	66.74 $\pm$ 10.04	33.26%	78.13 $\pm$ 4.07	21.87%	42.98 $\pm$ 4.46	57.02%	76.50 $\pm$ 4.58	23.50%
200	79.44 $\pm$ 1.60	20.56%	88.27 $\pm$ 2.61	11.73%	51.66 $\pm$ 2.99	48.34%	84.59 $\pm$ 5.22	15.41%
100	90.39 $\pm$ 1.45	9.61%	93.60 $\pm$ 2.10	6.4%	59.68 $\pm$ 1.54	40.32%	92.21 $\pm$ 2.78	7.79%
50	93.83 $\pm$ 1.29	6.17%	94.17 $\pm$ 1.57	5.83%	73.96 $\pm$ 1.73	26.04%	96.49 $\pm$ 1.29	3.51%
25	94.02 $\pm$ 2.63	5.98%	95.22 $\pm$ 0.82	4.78%	86.73 $\pm$ 1.30	13.27%	96.95 $\pm$ 1.14	3.05%
IC <sub>50</sub>	214.8		300.5		33.41		201.1	

healthy cells. By integrating MCF-7 cancer cells and WRL-68 normal cells separately with the prepared compounds at 5% CO<sub>2</sub> atmosphere and 37 °C temperature for 24 h at different concentrations ranging from 400–25 g/mL and using the ELISA device, the absorbance was calculated at the wavelength of 570 nm and using the statistical program and IC<sub>50</sub> calculation, the absorbance was calculated at the wavelength of 570 nm and by using the statistical program and IC<sub>50</sub> calculation. The ligand's effect on the MCF-7 cancer cell line was found to be less than that of the platinum complex, as it inhibited cells by 33.26, 20.56, 9.61, 6.17, and 5.98% at concentrations of 400, 200, 100, 50 and 25 g/mL, respectively. While at concentrations of 400–25 g/mL, it inhibited the normal cell line WRL-68 by 21.87–4.78%. The platinum complex performed better than the ligand, inhibiting MCF-7 cancer cells with a rate ranging between 57.02–13.27%, while inhibiting normal cells WRL-68 with a rate ranging between 23.5–3.05%. Table 6 and Fig. S14 and S15 show the percentages of inhibition as well as the IC<sub>50</sub> for each of the ligands and the platinum complex.

## ■ CONCLUSION

The measurements were used to determine the geometry of the compound (elementary analysis, electronic and atomic absorption spectroscopy, infrared spectroscopy, molar conductivity, and magnetic susceptibility experiments). These observations were also supported by the octahedral geometry of the Ni(II), Cu(II), and Pt(IV) complexes, as well as the tetrahedral geometry of the Ag(I) complexes. We concluded that the ligand and the Pt(IV) complex have high antioxidants

against free radicals after conducting applications and biological activity tests on the ligand and the prepared complexes. In addition, we discovered through MTT toxicity testing that they are highly effective against breast cancer MCF-7 cells. Through this research, it will be possible to work intensively and precisely on these proposed compounds in the future in order to benefit from them in the medical field and use them as anti-breast cancer drugs. It was also concluded that all compounds exhibit nanotechnology characteristics, indicating the position and direction of the world's view on these compounds, their importance, and their entry into many industrial, medical, and electronic fields.

## ■ REFERENCES

- [1] Miller, M.M., Vasiliadis, T., Rochman, C.M., Repich, K., Patrie, J.T., Anderson, R.T., and Harvey, J.A., 2023, Factors associated with perceived personal risk for breast cancer among women with dense breasts, *Clin. Imaging*, 93, 34–38.
- [2] Mathelin, C., Domínguez-Gil, B., Özmen, V., and Lodi, M., 2023, European guidelines concerning the transplantation of organs from donors with a history of breast cancer, *Eur. J. Breast Health*, 19 (1), 106–109.
- [3] Karademas, E.C., Roziner, I., Mazzocco, K., Pat-Horenczyk, R., Sousa, B., Oliveira-Maia, A.J., Stamatakis, G., Cardoso, F., Frasilho, D., Kolokotroni, E., Lemos, R., Marzorati, C., Mattson, J., Pettini, G., Spyropoulou, E., Poikonen-Saksela, P., and Simos, P., 2022, The mutual determination of self-efficacy to cope with cancer and cancer-

- related coping over time: A prospective study in women with breast cancer, *Psychol. Health*, 1–14.
- [4] Terrisse, S., Derosa, L., Iebba, V., Ghiringhelli, F., Vaz-Luis, I., Kroemer, G., Fidelle, M., Christodoulidis, S., Segata, N., Thomas, A.M., Martin, A.L., Sirven, A., Everhard, S., Aprahamian, F., Nirmalathasan, N., Aarnoutse, R., Smidt, M., Ziemons, J., Caldas, C., Loibl, S., Denkert, C., Durand, S., Iglesias, C., Pietrantonio, F., Routy, B., André, F., Pasolli, E., Delalogue, S., and Zitvogel, L., 2021, Intestinal microbiota influences clinical outcome and side effects of early breast cancer treatment, *Cell Death Differ.*, 28 (9), 2778–2796.
- [5] Scarim, C.B., and Chin, C.M., 2022, Recent trends in drug development for the treatment of adenocarcinoma breast cancer: Thiazole, triazole, and thiosemicarbazone analogues as efficient scaffolds, *Anti-Cancer Agents Med. Chem.*, 22 (12), 2204–2240.
- [6] Campana, L.G., Galuppo, S., Valpione, S., Brunello, A., Ghiotto, C., Ongaro, A., and Rossi, C.R., 2014, Bleomycin electrochemotherapy in elderly metastatic breast cancer patients: Clinical outcome and management considerations, *J. Cancer Res. Clin. Oncol.*, 140 (9), 1557–1565.
- [7] Özbek, O., and Gürdere, M.B., 2021, Synthesis and anticancer properties of 2-aminothiazole derivatives, *Phosphorus, Sulfur Silicon Relat. Elem.*, 196 (5), 444–454.
- [8] Alizadeh, S.R., and Hashemi, S.M., 2021, Development and therapeutic potential of 2-aminothiazole derivatives in anticancer drug discovery, *Med. Chem. Res.*, 30 (4), 771–806.
- [9] Minickaitė, R., Grybaitė, B., Vaickelionienė, R., Kavaliauskas, P., Petraitis, V., Petraitienė, R., Tumosienė, I., Jonuškienė, I., and Mickevičius, V., 2022, Synthesis of novel aminothiazole derivatives as promising antiviral, antioxidant and antibacterial candidates, *Int. J. Mol. Sci.*, 23 (14), 7688.
- [10] Ding, M., Wu, N., Lin, Q., Yan, Y., Yang, Y., Tian, G., An, L., and Bao, X., 2022, Discovery of novel quinazoline-2-aminothiazole hybrids containing a 4-piperidinylamide linker as potential fungicides against the phytopathogenic fungus *Rhizoctonia solani*, *J. Agric. Food Chem.*, 70 (33), 10100–10110.
- [11] Makam, P., and Kannan, T., 2014, 2-Aminothiazole derivatives as antimycobacterial agents: Synthesis, characterization, *in vitro* and *in silico* studies, *Eur. J. Med. Chem.*, 87, 643–656.
- [12] Farouk Elsadek, M., Mohamed Ahmed, B., and Fawzi Farahat, M., 2021, An overview on synthetic 2-aminothiazole-based compounds associated with four biological activities, *Molecules*, 26 (5), 1449.
- [13] Niu, Z.X., Wang, Y.T., Zhang, S.N., Li, Y., Chen, X.B., Wang, S.Q., and Liu, H.M., 2023, Application and synthesis of thiazole ring in clinically approved drugs, *Eur. J. Med. Chem.*, 250, 115172.
- [14] Ates, B., Koytepe, S., Ulu, A., Gurses, C., and Thakur, V.K., 2020, Chemistry, structures, and advanced applications of nanocomposites from biorenewable resources, *Chem. Rev.*, 120 (17), 9304–9362.
- [15] Razzaq, A.S., and Nahi, R.J., 2021, *In vitro*, evaluation of antioxidant and antibacterial activities of new 1,2,3-triazole derivatives containing 1,2,4-triazole ring, *Syst. Rev. Pharm.*, 12 (1), 196–200.
- [16] Kyhoiesh, H.A.K., and Al-Adilee, K.J., 2021, Synthesis, spectral characterization, antimicrobial evaluation studies and cytotoxic activity of some transition metal complexes with tridentate (N,N,O) donor azo dye ligand, *Results Chem.*, 3, 100245.
- [17] Charisiadis, P., Kontogianni, V.G., Tsiafoulis, C.G., Tzakos, A.G., Siskos, M., and Gerothanassis, I.P., 2014, <sup>1</sup>H-NMR as a structural and analytical tool of intra- and intermolecular hydrogen bonds of phenol-containing natural products and model compounds, *Molecules*, 19 (9), 13643–13682.
- [18] Mohammadi, K., and Zahedi, M., 2012, Tridentate Schiff base compounds of 2-aminophenol: Synthesis, characterization and complexation with IIIA elements, *Global J. Inorg. Chem.*, 3 (2), 1–12.
- [19] Raman, N., 2002, Synthesis, structural characterization, redox and antimicrobial studies of Schiff base copper(II), nickel(II), cobalt(II), manganese(II), zinc(II) and oxovanadium(II) complexes derived from benzil and 2-aminobenzyl

- alcohol, *Pol. J. Chem.*, 76 (8), 1085–1094.
- [20] Abouzied, A.S., Break, M.K.B., Huwaimel, B., Hussein, W., Alafnan, A., and Younes, K.M., 2023, Discovery of a novel synthetic thiazole-benzimidazole conjugate that acts as a potent pancreatic lipase inhibitor using *in silico* and *in vitro* approaches, *Indian J. Pharm. Educ. Res.*, 57 (1), 218–227.
- [21] Emadi, A., 2020, Schiff benzimidazole derivatives: synthesis, properties and antimicrobial activity, *Int. J. Farming Allied Sci.*, 9, 72–82.
- [22] Çakmak, Ş., Koşar Kırca, B., Veyisoğlu, A., Yakan, H., Ersanlı, C.C., and Kütük, H., 2022, Experimental and theoretical investigations on a furan-2-carboxamide-bearing thiazole: Synthesis, molecular characterization by IR/NMR/XRD, electronic characterization by DFT, Hirshfeld surface analysis and biological activity, *Acta Crystallogr., Sect. C: Struct. Chem.*, 78 (3), 201–211.
- [23] More, R.M., Kadam, A.B., Dalvi, S.P., Humne, V.T., and Junne, S.B., 2022, Synthesis, characterization and anti-bacterial activity of Schiff base hybrid from 2-aminothiazole-pyrazolecarboxaldehyde, *J. Adv. Chem. Sci.*, 8 (4), 781–783.
- [24] Rathnayaka, C., George, S., Abeysinghe, J.P., Lynch, V.M., and Gross, D.E., 2022, Synthetic, spectroscopic, and computational investigations of readily accessible 2-phenyl-3-alkylbenzoxazaboroles, *J. Heterocycl. Chem.*, 59 (6), 1036–1044.
- [25] Zelelew, D., Endale, M., Melaku, Y., Kedir, F., Demissie, T.B., Ombito, J.O., and Eswaramoorthy, R., 2022, Synthesis, anti-bacterial, and antioxidant activities of thiazolyl-pyrazoline Schiff base hybrids: A combined experimental and computational study, *J. Chem.*, 2022, 3717826.
- [26] Duc, D.X., and Lanh, H.T., 2022, Microwave-assisted, [Bmim]HSO<sub>4</sub>-catalyzed synthesis of tetrasubstituted imidazoles via four-component reaction, *Vietnam J. Sci. Technol.*, 60 (3), 383–390.
- [27] Al-Jibouri, M.N., Hafidh, F.R., and Rasheed, A.M., 2014, Synthesis and characterization of some transition metal complexes with tridentate N<sub>3</sub> donor Schiff base derived from 2-aminothiazole, *Eur. Chem. Bull.*, 3 (6), 559–562.
- [28] Camellia, F.K., Ashrafuzzaman, M., Islam, M.N., Banu, L.A., and Zahan, M.K.E., 2022, Isoniazid derived Schiff base metal complexes: Synthesis, characterization, thermal stability, anti-bacterial and antioxidant activity study, *Asian J. Chem. Sci.*, 11 (4), 23–36.
- [29] Al-Amery, H., Al-Abdaly, B.I., and Albayaty, M.K., 2016, Synthesis, characterization and anti-bacterial activity of new complexes of some lanthanide ions with 15-crown-5 and 18-crown-6, *Orient. J. Chem.*, 32 (2), 1025–1048.
- [30] Abdel-Rahman, L.H., Adam, M.S.S., Al-Zaqri, N., Shehata, M.R., Ahmed, H.E.S., and Mohamed, S.K., 2022, Synthesis, characterization, biological and docking studies of ZrO(II), VO(II) and Zn(II) complexes of a halogenated tetra-dentate Schiff base, *Arabian J. Chem.*, 15 (5), 103737.
- [31] Gul, Z., Din, N.U., Khan, E., Ullah, F., and Nawaz Tahir, M., 2020, Synthesis, molecular structure, anti-microbial, antioxidant and enzyme inhibition activities of 2-amino-6-methylbenzothiazole and its Cu(II) and Ag(I) complexes, *J. Mol. Struct.*, 1199, 126956.
- [32] Barfeie, H., Grivani, G., Eigner, V., Dusek, M., and Khalaji, A.D., 2018, Copper(II), nickel(II), zinc(II) and vanadium(IV) Schiff base complexes: Synthesis, characterization, crystal structure determination, and thermal studies, *Polyhedron*, 146, 19–25.
- [33] Thakar, A., Joshi, K., Pandya, K., and Pancholi, A., 2011, Coordination modes of a Schiff base derived from substituted 2-aminothiazole with chromium(III), manganese(II), iron(II), cobalt(II), nickel(II) and copper(II) metal ions: Synthesis, spectroscopic and antimicrobial studies, *J. Chem.*, 8, 282061.
- [34] Daravath, S., Kumar, M.P., Rambabu, A., Vamsikrishna, N., Ganji, N., and Shivaraj, S., 2017, Design, synthesis, spectral characterization, DNA interaction and biological activity studies of copper(II), cobalt(II) and nickel(II) complexes of 6-amino benzothiazole derivatives, *J. Mol. Struct.*, 1144, 147–158.
- [35] Swami, S., Sharma, N., Agarwala, A., Shrivastava, V.,

- and Shrivastava, R., 2021, Schiff base anchored silver nanomaterial: An efficient and selective nano probe for fluoride detection in an aqueous medium, *Mater. Today: Proc.*, 43, 2926–2932.
- [36] Adnan, S., Al-Adilee, K.J., and Abedalrazaq, K.A., 2020, Synthesis, spectral characterization and anticancer studies of novel azo Schiff base and its complexes with Ag(I), Au(III) and Pt(IV) ions, *Egypt. J. Chem.*, 63 (12), 4749–4756.
- [37] Elkanzi, N.A., Hrichi, H., Salah, H., Albqmi, M., Ali, A.M., and Abdou, A., 2023, Synthesis, physicochemical properties, biological, molecular docking and DFT investigation of Fe(III), Co(II), Ni(II), Cu(II) and Zn(II) complexes of the 4-[(5-oxo-4,5-dihydro-1,3-thiazol-2-yl)hydrazono]methyl} phenyl 4-methylbenzenesulfonate Schiff-base ligand, *Polyhedron*, 230, 116219.
- [38] Rajmane, S., Ubale, V.P., Dama, L.B., Asabe, M.R., and More, P.G., 2013, Synthesis, spectral and biological studies of thiazole Schiff base derived from 4-(2'-fluorophenyl)-2-aminothiazole, *Int. J. Pharm. Sci. Invent.*, 2 (7), 33–36.